

6-10-2022

## Intraneuronal $\beta$ -amyloid Accumulation: Aging HIV-1 Human and HIV-1 Transgenic Rat Brain

Hailong Li

Kristen A. McLaurin

Charles F. Mactutus

Benjamin Linkins

Wenfei Huang

*See next page for additional authors*

Follow this and additional works at: [https://scholarcommons.sc.edu/psyc\\_facpub](https://scholarcommons.sc.edu/psyc_facpub)



Part of the [Psychology Commons](#)

---

### Publication Info

Published in *Viruses*, Volume 14, Issue 6, 2022, pages 1268-

© 2022 by the authors. Licensee MDPI, Basel, Switzerland. This article is an open access article distributed under the terms and conditions of the Creative Commons Attribution (CC BY) license(<https://creativecommons.org/licenses/by/4.0/>).

This Article is brought to you by the Psychology, Department of at Scholar Commons. It has been accepted for inclusion in Faculty Publications by an authorized administrator of Scholar Commons. For more information, please contact [digres@mailbox.sc.edu](mailto:digres@mailbox.sc.edu).



---

**Author(s)**

Hailong Li, Kristen A. McLaurin, Charles F. Mactutus, Benjamin Linkins, Wenfei Huang, Sulie L. Chang, and Rosemarie M. Booze

## Article

# Intraneuronal $\beta$ -Amyloid Accumulation: Aging HIV-1 Human and HIV-1 Transgenic Rat Brain

Hailong Li <sup>1</sup>, Kristen A. McLaurin <sup>1</sup>, Charles F. Mactutus <sup>1</sup>, Benjamin Likins <sup>1</sup>, Wenfei Huang <sup>2,3</sup>,  
Sulie L. Chang <sup>2,3</sup>  and Rosemarie M. Booze <sup>1,\*</sup> 

<sup>1</sup> Department of Psychology, University of South Carolina, Columbia, SC 29208, USA; hailong@mailbox.sc.edu (H.L.); mclaurik@email.sc.edu (K.A.M.); mactutus@mailbox.sc.edu (C.F.M.); likins@musc.edu (B.L.)

<sup>2</sup> Institute of NeuroImmune Pharmacology, Seton Hall University, South Orange, NJ 07079, USA; wenfei.huang@shu.edu (W.H.); sulie.chang@shu.edu (S.L.C.)

<sup>3</sup> Department of Biological Sciences, Seton Hall University, South Orange, NJ 07079, USA

\* Correspondence: booze@mailbox.sc.edu

**Abstract:** The prevalence of HIV-1 associated neurocognitive disorders (HAND) is significantly greater in older, relative to younger, HIV-1 seropositive individuals; the neural pathogenesis of HAND in older HIV-1 seropositive individuals, however, remains elusive. To address this knowledge gap, abnormal protein aggregates (i.e.,  $\beta$ -amyloid) were investigated in the brains of aging (>12 months of age) HIV-1 transgenic (Tg) rats. In aging HIV-1 Tg rats, double immunohistochemistry staining revealed abnormal intraneuronal  $\beta$ -amyloid accumulation in the prefrontal cortex (PFC) and hippocampus, relative to F344/N control rats. Notably, in HIV-1 Tg animals, increased  $\beta$ -amyloid accumulation occurred in the absence of any genotypic changes in amyloid precursor protein (APP). Furthermore, no clear amyloid plaque deposition was observed in HIV-1 Tg animals. Critically,  $\beta$ -amyloid was co-localized with neurons in the cortex and hippocampus, supporting a potential mechanism underlying synaptic dysfunction in the HIV-1 Tg rat. Consistent with these neuropathological findings, HIV-1 Tg rats exhibited prominent alterations in the progression of temporal processing relative to control animals; temporal processing relies, at least in part, on the integrity of the PFC and hippocampus. In addition, in post-mortem HIV-1 seropositive individuals with HAND, intraneuronal  $\beta$ -amyloid accumulation was observed in the dorsolateral PFC and hippocampal dentate gyrus. Consistent with observations in the HIV-1 Tg rat, no amyloid plaques were found in these post-mortem HIV-1 seropositive individuals with HAND. Collectively, intraneuronal  $\beta$ -amyloid aggregation observed in the PFC and hippocampus of HIV-1 Tg rats supports a potential factor underlying HIV-1 associated synaptodendritic damage. Further, the HIV-1 Tg rat provides a biological system to model HAND in older HIV-1 seropositive individuals.

**Keywords:**  $\beta$ -amyloid; prepulse inhibition; RNAscope; neurodegenerative diseases; HIV-1



**Citation:** Li, H.; McLaurin, K.A.; Mactutus, C.F.; Likins, B.; Huang, W.; Chang, S.L.; Booze, R.M. Intraneuronal  $\beta$ -Amyloid Accumulation: Aging HIV-1 Human and HIV-1 Transgenic Rat Brain. *Viruses* **2022**, *14*, 1268. <https://doi.org/10.3390/v14061268>

Academic Editors: Samantha S. Soldan and Cagla Akay-Espinoza

Received: 12 April 2022

Accepted: 7 June 2022

Published: 10 June 2022

**Publisher's Note:** MDPI stays neutral with regard to jurisdictional claims in published maps and institutional affiliations.



**Copyright:** © 2022 by the authors. Licensee MDPI, Basel, Switzerland. This article is an open access article distributed under the terms and conditions of the Creative Commons Attribution (CC BY) license (<https://creativecommons.org/licenses/by/4.0/>).

## 1. Introduction

The life expectancy of individuals living with human immunodeficiency virus type 1 (HIV-1) dramatically increased following the advent of combination antiretroviral therapy (cART; [1,2]). Indeed, HIV-1 seropositive individuals 50 years of age and older account for approximately 30–50% of all HIV-1 seropositive individuals in high-resource countries [3]; a prevalence which is expected to reach 73% by 2030 [4]. Critically, older HIV-1 seropositive individuals exhibit a higher frequency of neurocognitive deficits relative to their younger counterparts [5–7] underscoring the importance of an investigation of the neuropathological mechanisms underlying these disorders.

Synaptodendritic damage [8,9] and spine dysmorphology/loss [10–12] have been implicated as key neural mechanisms underlying HAND in HIV-1 seropositive individuals. Fundamentally, synaptic damage, measured using the presynaptic protein synaptophysin

and/or the dendritic microtubule activation protein 2, correlates with the severity of neurocognitive impairments [8,13]. Furthermore, multiple biological systems utilized to model HAND exhibit prominent synaptodendritic damage and/or spine dysmorphology/loss (e.g., Tat transgenic (Tg) mice: [14,15]; gp120 Tg mice: [16,17]; HIV-1 Tg rat: [18–21]; chimeric HIV rat: [22]); alterations that generalize across brain regions (e.g., prefrontal cortex (PFC), nucleus accumbens (NAc), and hippocampus) and ages (e.g., 4 months, 14–17 months, and 20 months of age). However, the factors underlying (e.g.,  $\beta$ -amyloid) HIV-1 associated synaptodendritic damage remain elusive [23,24].

Toxic  $\beta$ -amyloid proteins have deleterious effects on neurons, including synaptodendritic loss and spine dysmorphology (e.g., [25,26]) affording a potential mechanism underlying synaptodendritic damage in HIV-1.  $\beta$ -amyloid proteins are formed following the proteolysis of the amyloid precursor protein (APP) along either the nonamyloidogenic or the amyloidogenic pathway (for review, [27]). First, APP is cleaved by either  $\alpha$ - (non-amyloidogenic) or  $\beta$ - (amyloidogenic) secretase releasing soluble APP $\alpha$  and soluble APP $\beta$ , respectively, from the cell surface. C-terminal fragments of either 83-amino acids ( $\alpha$ -secretase; C83) or 99-amino acids ( $\beta$ -secretase; C99) afford substrates for  $\gamma$ -secretase. During amyloidogenic processing, the cleavage of C99 by  $\gamma$ -secretase yields either extracellular  $\beta$ -amyloid peptides of varying lengths (e.g., 51–30 amino acid residues) or the APP intracellular domain. Further cleavage of  $\beta$ -amyloid peptides results in the generation of the main final forms of  $\beta$ -amyloid, including  $\beta$ -amyloid<sub>40</sub> (A $\beta$ 40) and  $\beta$ -amyloid<sub>42</sub> (A $\beta$ 42; [28,29]). Although A $\beta$ 40 is the most abundant isoform in the brain [30], A $\beta$ 42 is predominant in neuritic plaques (e.g., [31,32]).

Thus, the present study investigated protein aggregates (i.e.,  $\beta$ -amyloid) as a potential neuropathological mechanism underlying synaptic dysfunction in HIV-1. First,  $\beta$ -amyloid protein aggregates were assessed in the brains of aging (>12 months of age) HIV-1 transgenic (Tg) and F344/N control rats. The HIV-1 Tg rat expresses seven of the nine HIV-1 genes (deletion of the *pol* and *gag* genes) constitutively throughout development [33] and affords a biological system to model age-related disease progression [20]. Second, the nature of  $\beta$ -amyloid accumulation (i.e., intraneuronal vs. extracellular plaques) was examined in the post-mortem brains of HIV-1 seropositive individuals with HAND. Examination of  $\beta$ -amyloid protein accumulation and its co-localization with neurons affords an opportunity to understand the fundamental factors underlying HIV-1 associated synaptodendritic damage.

## 2. Materials and Methods

### 2.1. Experiment 1: HIV-1 Transgenic Rats

All animals were housed and cared for in AAALAC-accredited facilities according to guidelines established by the National Institutes of Health. The protocols were approved by the Institutional Animal Care and Use Committee (IACUC) at the University of South Carolina (Federal Assurance #D16-00028).

#### 2.1.1. Neuroanatomical Assessments

##### Animals

Aging (>12 months of age) Fischer HIV-1 Tg rats and F344/N control rats were pair-housed in a controlled environment. F344/N control animals were procured from Envigo Laboratories (Indianapolis, IN, USA), whereas HIV-1 Tg animals were bred by housing a control female and HIV-1 Tg male together at the University of South Carolina. Animals were maintained under a 12:12 light/dark cycle with ad libitum access to food (Pro-Lab Rat, Mouse, Hamster Chow #3000) and water.

##### Immunofluorescence Staining

Animals (HIV-1 Tg: male,  $n = 4$ ; female,  $n = 4$ ; F344/N Control: male,  $n = 4$ ; female,  $n = 4$ ) were deeply anesthetized using sevoflurane (Abbot Laboratories, North Chicago, IL, USA) and transcardially perfused with 4% paraformaldehyde. After perfusion, brains

were removed, post-fixed overnight in 4% chilled paraformaldehyde, and sectioned using a vibratome (100  $\mu\text{m}$  thick coronal slices). Brain sections were incubated with either the Alexa Fluor<sup>®</sup> 488 anti-beta Amyloid 1-42 rabbit monoclonal antibody (Cat. No. ab224026, Abcam, Waltham, MA, USA), Alexa Fluor<sup>®</sup> 594 anti-NeuN rabbit monoclonal antibody (Cat. No. ab207279, Abcam, Waltham, MA, USA), or anti-Amyloid Precursor Protein rabbit monoclonal antibody (Cat. No. ab208744, Abcam, Waltham, MA, USA). Fluorescent images were acquired using a Nikon D-Eclipse C1 inverted fluorescence microscope. Analyses were conducted by evaluating the intensity of immunohistochemistry (IHC) staining using NIS-Elements BR3.10 software (Nikon, Melville, NY, USA), whereby the experimenter was blind to both genotype and sex.

### Neuronal Labeling

Methodological details for ballistic labeling were previously described in detail [34]. Briefly, Tefzel tubing (IDEX Health Sciences, Oak Harbor, WA, USA) was coated with polyvinylpyrrolidone (PVP). DiOlistic cartridges were prepared using 170 mg tungsten beads (Bio-Rad, Hercules, CA, USA) and lipophilic dye DiI (Invitrogen, Carlsbad, CA, USA), which were dissolved in 99.5% pure methylene chloride (Sigma-Aldrich, St. Louis, MO, USA), and mixed thoroughly. Approximately 100  $\mu\text{L}$  of the bead solution was pipetted onto a standard glass slide and 150  $\mu\text{L}$  DiI was added on top. The air dried bead/dye mixture was suspended in deionized  $\text{H}_2\text{O}$ , sonicated to homogenize, added to the PVP-coated Tefzel tubing, and dried under a nitrogen flow (0.4 LPM) for 30 min. Finally, the Helios gene gun (Bio-Rad, Hercules, CA, USA) was loaded with the previously prepared PVP-coated Tefzel tubing cartridges. The DiI/tungsten beads within the cartridges were delivered to the tissue sections using the Helios gene gun system. Helium gas pressure was set to 100 psi and brain slices were placed approximately 2.5 cm away from the barrel of the Helios gene gun. DiOlistically labeled tissue sections were mounted onto glass slides using Pro-Long Gold Antifade reagent (Cat. No. D1306, Fisherscience, MA, USA), coverslipped, and stored in the dark at 4  $^{\circ}\text{C}$ . Confocal images were obtained within 48 h of DiOlistic labeling.

### 2.1.2. Neurocognitive Assessments

#### Animals

Gap-prepulse inhibition (gap-PPI), tapping the cognitive domain of temporal processing, was evaluated in Fischer F344/N ( $n = 20$  litters) and HIV-1 Tg ( $n = 17$  litters) animals. Animals were procured in litters (F344/N Control,  $n = 20$  litters; HIV-1 Tg,  $n = 17$  litters) from Harlan Laboratories, Inc. (Indianapolis, IN, USA), arriving at the animal colony between postnatal day (PD) 7 and PD 9. HIV-1 Tg and control animals were sampled from each litter, yielding, HIV-1 Tg: male,  $n = 37$ , female,  $n = 33$  and Control: male  $n = 34$ ; female,  $n = 33$ . Animals (HIV-1 Tg:  $n = 14$ ; Control:  $n = 10$ ) exhibiting health issues were humanely sacrificed prior to the completion of the study. Animals were placed on food restriction at approximately PD 60, with the goal of maintaining approximately 85% body weight, during the beginning of a concurrently run operant task. Once animals successfully acquired the operant task (PD 100-PD 277), rodent food (Pro-Lab Rat, Mouse, Hamster Chow #3000) was available ad libitum. Water was available ad libitum.

#### Apparatus

The startle platform (SR-Lab Startle Reflex System, San Diego Instruments, Inc., San Diego, CA, USA) was enclosed in an isolation cabinet (external dimensions: 10 cm thick, double-walled, 81  $\times$  81  $\times$  116-cm; Industrial Acoustic Company, Inc., Bronx, NY, USA) that afforded sound attenuation (30 db(A)) relative to the external environment. Within the testing chamber, the ambient sound level was 22 db(A). Thirty cm above the Plexiglas test cylinder was a high-frequency loudspeaker of the SR-Lab system (model#40-1278B, Radio Shack, Fort Worth, TX, USA), which was utilized for the delivery of all auditory stimuli. Deflections of the Plexiglas test cylinder were converted into analog signals based

on a piezoelectric accelerometer attached to the bottom of the cylinder. Following the digitation (12 bit A to D, recorded at a rate of 2000 samples/sec) of response signals, they were saved to a hard disk. The SR-LAB Startle Calibration System was utilized to calibrate response sensitivities.

### Procedure

A longitudinal experimental design was utilized to assess the progression of temporal processing using the gap-prepulse inhibition experimental paradigm. HIV-1 Tg and control animals were tested for gap-PPI of the auditory startle response beginning at PD 240. Assessments were conducted every 60 days through PD 540. The methodology for the assessment of gap-PPI is similar to our prior publication [35]. In brief, the test session, which was approximately 20 min in duration, began with a 5 min acclimation period in the dark with 70 db(A) background white noise. Subsequently, six pulse-only ASR trials were utilized for habituation and separated by a 10 sec intertrial interval (ITI). Thirty-six testing trials were presented in six-trial blocks interdigitated using a Latin Square experimental design with a variable ITI (15–25 s. A 20 msec gap in background white noise preceded the auditory startle stimulus (100 db(A) intensity with a 20 msec duration) at interstimulus intervals (ISIs) of 30, 50, 100, and 200 msec. The gap-PPI assessment included two control trials, including both the 0 and 4000 msec ISI, providing a reference ASR within the assessment. Analyses were conducted on the peak ASR amplitude values.

### 2.2. Experiment 2: Post-Mortem HIV-1 Seropositive Individuals with HAND

Autopsy human brain tissues ( $n = 9$ ) were provided by the National NeuroAIDS Tissue Consortium (NNTC). Study participants were HIV-1 seropositive individuals with symptomatic HAND that had tissue samples from both the dorsolateral prefrontal cortex (dlPFC; Brodmann's Area 9 [36];  $n = 9$ ) and hippocampus (dentate gyrus;  $n = 3$ ). Participants died between 55 and 74 years of age. Additional demographic information is available in Supplementary Table S1. The NNTC Data Coordinating Center (DCC) approved the specimen application (Request # R703).

#### 2.2.1. Neuroanatomical Assessments

##### Immunofluorescence Staining

Human brain tissues were sectioned using a cryostat (50  $\mu\text{m}$  thick coronal slices) and incubated overnight at 4 °C with either the Alexa Fluor<sup>®</sup> 488 Anti-beta Amyloid 1-42 antibody (Cat. No. ab224026, Abcam, Waltham, MA, USA), Alexa Fluor<sup>®</sup> 594 Anti-NeuN antibody (Cat. No. ab207279, Abcam, Waltham, MA, USA), or PE Anti-Amyloid Precursor Protein antibody (Cat. No. ab208744, Abcam, Waltham, MA, USA). Fluorescent images were acquired using a Nikon D-Eclipse C1 inverted fluorescence microscope. The fluorescence signal was analyzed using NIS-Elements BR3.10 software.

##### Thioflavin-S Staining

Brain sections were immersed in a 1% Thioflavin-S (Cat. No. T1892, MilliporeSigma, Burlington, MA, USA) solution for 2 min at room temperature and differentiated in 70% ethanol until the sections were clear. Sections were washed with deionized water and mounted with Pro-Long Gold Antifade reagent.

### 2.3. Statistical Analysis

Data were analyzed using independent samples *t*-test (SPSS Statistics 27, IBM Corp., Somers, NY, USA), analysis of variance (ANOVA; SPSS Statistics 27), or regression statistical techniques (GraphPad Prism 5.02, GraphPad Software, Inc., La Jolla, CA, USA). Figures were created using GraphPad Prism 5. Statistical significance was established at an alpha level of  $p \leq 0.05$ . Partial eta squared ( $\eta_p^2$ ) is presented as a measure of effect size.

IHC intensity data for  $\beta$ -amyloid or APP were analyzed using an ANOVA, whereby genotype (HIV-1 Tg versus Control) and sex (male versus female) served as between-



subjects factors. The measured intensity of  $\beta$ -amyloid in the hippocampal CA3 region was transformed using a square root transformation.

The progression of temporal processing was analyzed using regression statistical techniques. Given the nested experimental design (i.e., rats within litters), individual observations were analyzed using litter means and standard errors, dependent upon biological sex. Additionally, the mean series imputation method was used for all censored data.

### 3. Results

#### 3.1. Experiment 1: HIV-1 Transgenic Rats

##### 3.1.1. Neuroanatomical Assessments

IHC (Figure 1) was used to detect the expression of  $\beta$ -amyloid and APP in the medial prefrontal cortex (mPFC) and hippocampal CA3 region of aging HIV-1 Tg and F344/N control rats. With regards to  $\beta$ -amyloid, HIV-1 Tg animals exhibited abnormal accumulation in both the mPFC (main effect of genotype:  $F(1,15) = 12.6$ ,  $p \leq 0.004$ ,  $\eta_p^2 = 0.513$ ) and hippocampal CA3 region (main effect of genotype:  $F(1,15) = 5.1$ ,  $p \leq 0.044$ ,  $\eta_p^2 = 0.296$ ) relative to F344/N control rats (Figure 1D). With regards to APP, no statistically significant genotype and/or sex differences ( $p > 0.05$ ) were observed in either the mPFC or CA3 region of hippocampus (Figure 1E).

Furthermore, two methods (i.e., IHC double staining and DiOlistic labeling) were utilized to evaluate the location of  $\beta$ -amyloid accumulated. First, double staining of  $\beta$ -amyloid and NeuN, a neuronal marker, supports a strong co-localization of  $\beta$ -amyloid signals and neurons in both the mPFC and hippocampal region (Figure 1A,B). Second, DiOlistic labeling was also performed using ballistic techniques to confirm the co-localization between  $\beta$ -amyloid and hippocampal and/or cortical neurons (Figure 2); observations which further support  $\beta$ -amyloid accumulation as a potential mechanism underlying synaptic alterations in the HIV-1 Tg rat.

##### 3.1.2. Neurocognitive Assessments

In gap-PPI, the area of the inflection of the ASR response curve (a measure of prepulse inhibition), was utilized to examine the progression of temporal processing in HIV-1 Tg and control rats from PD 240 to PD 540 (Figure 3). HIV-1 Tg animals, relative to controls, displayed a prominent alteration in the progression of temporal processing (Figure 3A). For control animals, a segmental linear regression provided a well-described fit, with a linear increase in maximal prepulse inhibition observed through approximately PD 300, followed by a subsequent decline ( $R^2 = 0.85$ ). In sharp contrast, a first-order polynomial with a negative slope (i.e.,  $\beta_1 = -392.9 \pm 239.6$  ( $X \pm 95\%$  confidence interval)) provided a well-described fit for HIV-1 Tg rats ( $R^2 = 0.83$ ). The magnitude of alterations in the progression of temporal processing, however, was significantly influenced by the factor of biological sex (Figure 3B,C).

Complementary analyses of each genotype were conducted to determine the locus of these interactions. In male rats (Figure 3B), a segmental linear regression provided a well-described fit for control animals ( $R^2 = 0.76$ ) with maximal inhibition observed at PD 300, followed by a subsequent decline. Temporal processing in male HIV-1 Tg rats, however, was well-described by a first-order polynomial with a negative slope  $R^2 = 0.96$ ;  $\beta_1 = -392.9 \pm 344.12$  ( $X \pm 95\%$  confidence interval)). In female rats (Figure 3C), a first-order polynomial provided an appropriate fit for the development of temporal processing in control rats ( $R^2 = 0.87$ ). However, female HIV-1 Tg rats failed to exhibit any significant development in temporal processing from PD 240 to PD 540, evidenced by a horizontal fit. Aging HIV-1 Tg rats, therefore, displayed prominent alterations in the progression of temporal processing, with more significant deficits observed in female rats.

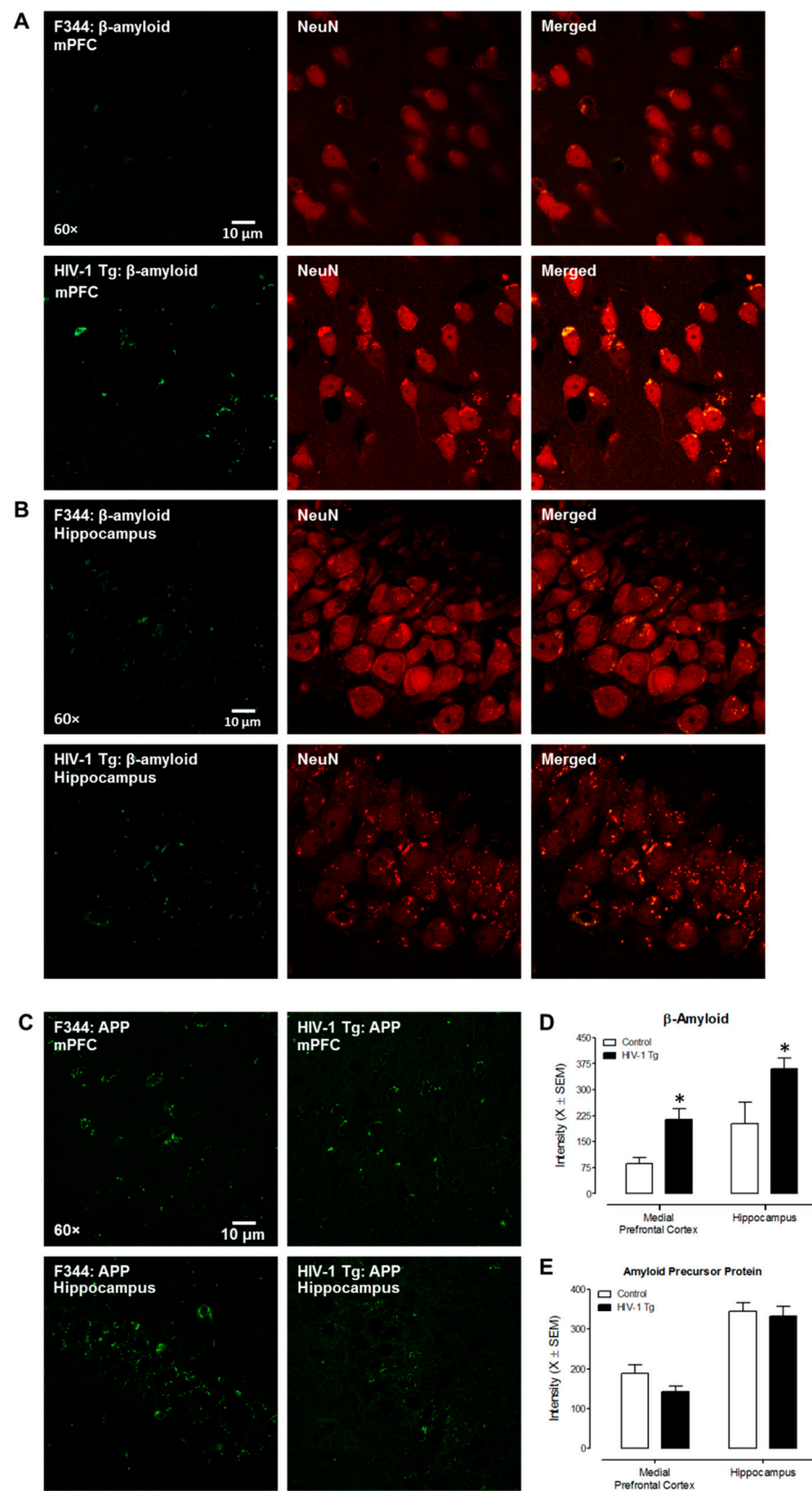


**Figure 1.** IHC double staining revealed an abnormal intraneuronal accumulation of  $\beta$ -amyloid in the HIV-1 Tg rat. (A,B) Representative confocal images of  $\beta$ -amyloid expression and co-localization with NeuN (neuronal marker) in the mPFC and CA3 area of hippocampus in F344/N and HIV-1 Tg rats. The Alexa 488 green fluorescence indicates expression of  $\beta$ -amyloid; the Alexa 594 red fluorescence



represents NeuN signals. (C) Representative images of amyloid precursor protein (APP) expression in the mPFC and hippocampal CA3 region in HIV-1 Tg and F344/N rats. APP expression is indicated by green fluorescence. (D) HIV-1 Tg rats exhibited abnormal accumulation of  $\beta$ -amyloid in both the mPFC and hippocampal CA3 region relative to control animals. (E) Statistical evaluation of APP in the mPFC and hippocampal CA3 areas compared to control rat. Statistically significant ( $p \leq 0.05$ ) differences between HIV-1 Tg and control animals are indicated using an \*.

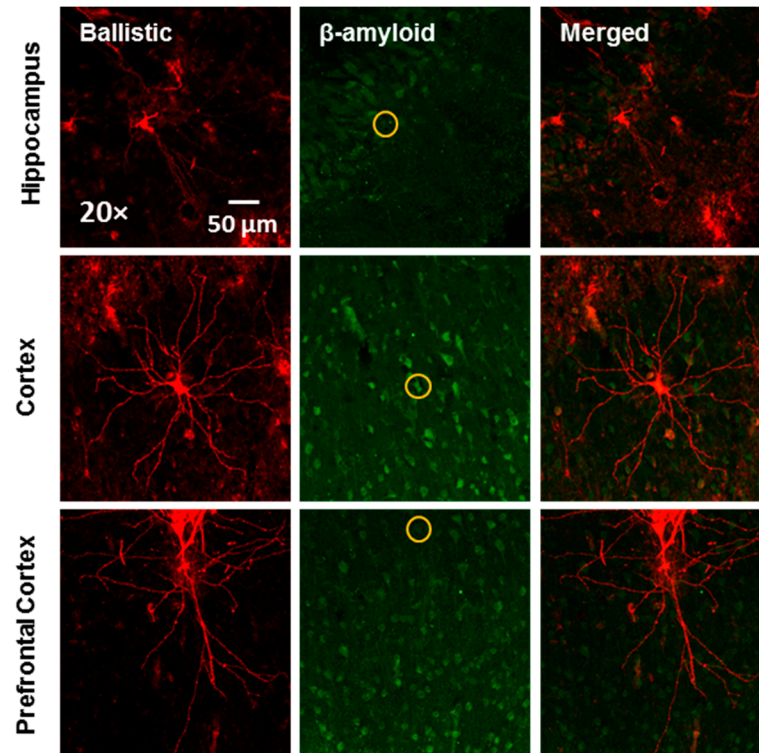


**Figure 2.** Co-localization of DiOlistically labeled neurons and  $\beta$ -amyloid immunostaining in the hippocampus, cortex, and prefrontal cortex. The yellow circle indicated the DiOlistically labeled neuron co-localizing with  $\beta$ -amyloid immunostaining positive signal

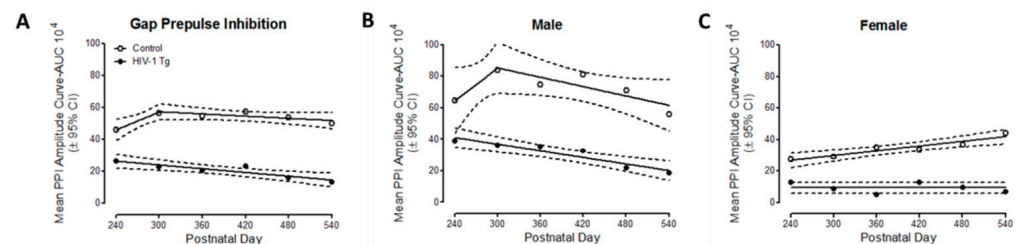


**Figure 3.** Neurocognitive assessments of temporal processing were evaluated using gap-prepulse inhibition (gap-PPI). The mean peak ASR amplitude response curve for gap-PPI was used to calculate prepulse inhibition in HIV-1 Tg and control rats from PD 240 to PD 540. (A) At the genotypic level, HIV-1 Tg animals exhibited a profound alteration in the progression of temporal processing relative to control animals. (B,C) Fundamentally, both male (B) and female (C) HIV-1 Tg animals displayed prominent alterations in the progression of temporal processing; the magnitude of these alterations was influenced by biological sex.

### 3.2. Experiment 2: Post-Mortem HIV-1 Seropositive Individuals with HAND

The nature of  $\beta$ -amyloid accumulation (i.e., intraneuronal vs. extracellular plaques) was examined in the dorsolateral PFC (Area 9,  $n = 9$ ) and hippocampal dentate gyrus

( $n = 3$ ) of post-mortem HIV-1 seropositive individuals with HAND. Both  $\beta$ -amyloid 1-42 and APP were observed in the dIPFC and hippocampus of HIV-1 seropositive individuals (Figure 4). Critically, there was no significant  $\beta$ -amyloid plaque deposition in either the dIPFC or hippocampus, evidenced by the absence of thioflavin-s staining. Meanwhile, the double staining of  $\beta$ -amyloid with NeuN (a neuronal marker) suggested that  $\beta$ -amyloid accumulation occurred intraneuronally. Collectively, aged HIV-infected individuals with HAND exhibited intraneuronal  $\beta$ -amyloid accumulation in the absence of any significant  $\beta$ -amyloid plaques.

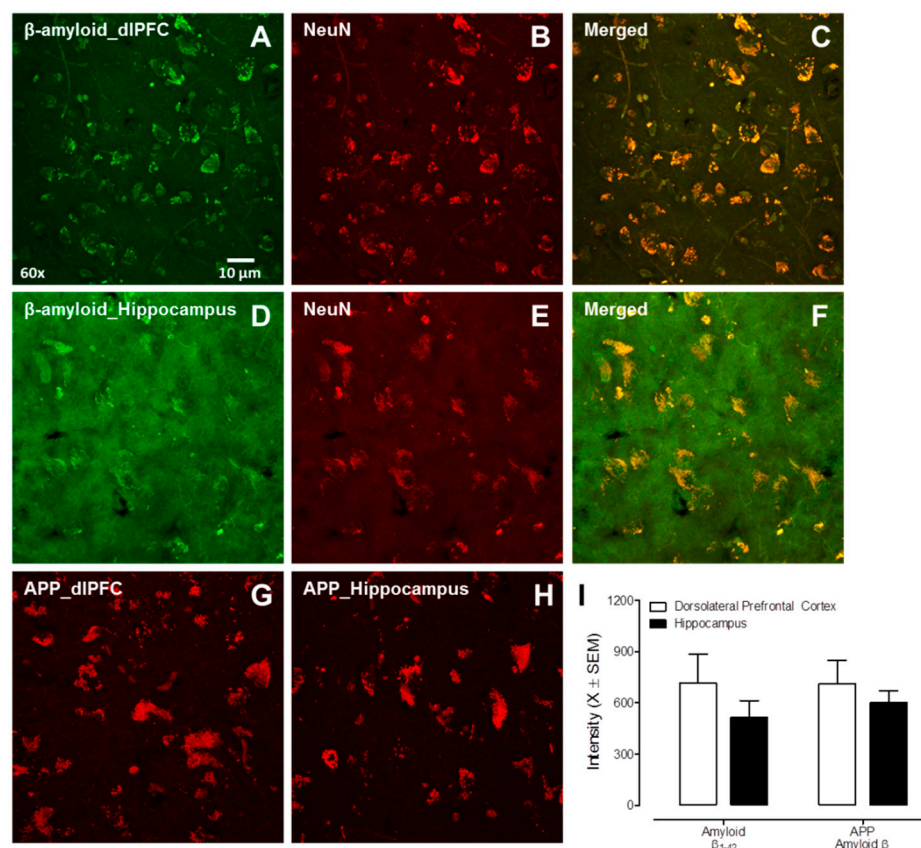


**Figure 4.**  $\beta$ -amyloid accumulation in the dorsolateral PFC (dIPFC) and hippocampal dentate gyrus from human autopsy HIV-infected cases with HAND. (A–F) Representative images of double staining of  $\beta$ -amyloid with NeuN (a neuronal marker) in the dIPFC (A–C), and in the hippocampus from human autopsy (D–F). (G,H) Confocal images of amyloid precursor protein expression in the dIPFC and hippocampus. (I) Quantification of  $\beta$ -amyloid and amyloid precursor protein expression in the dIPFC and hippocampus.

#### 4. Discussion

Intraneuronal  $\beta$ -amyloid accumulation was observed in the frontal cortex and hippocampus in both HIV-1 Tg rats and HIV-1 seropositive individuals with HAND. Notably, in HIV-1 Tg rats, increased  $\beta$ -amyloid accumulation occurred in the absence of any genotypic changes in APP. Consistent with these neuropathological findings, HIV-1 Tg rats exhibited prominent alterations in cognitive processes (i.e., temporal processing) dependent upon hippocampal and PFC function. Critically, the intraneuronal nature of  $\beta$ -amyloid accumulation in HIV-1 seropositive individuals is consistent with previous reports (e.g., [37,38]) and resembled observations in the HIV-1 Tg rat. Collectively, intraneuronal  $\beta$ -amyloid accumulation observed in the frontal cortex and hippocampus of both HIV-1 seropositive individuals and the HIV-1 Tg rat supports a potential factor underlying the HIV-1 associated synaptodendritic alterations.

HIV-1 viral proteins may underlie the abnormal intraneuronal accumulation of  $\beta$ -amyloid. Specifically, HIV-1 viral proteins may alter  $\beta$ -amyloid synthesis and/or  $\beta$ -amyloid degradation [23,38–40]; alterations that would decrease the clearance of  $\beta$ -amyloid. First, the HIV-1 transactivator of transcription (tat) and envelope glycoprotein gp120 (gp120) may promote the synthesis, secretion, and accumulation of  $\beta$ -amyloid [23,39]. Second, tat and/or tat-derived peptides may inhibit neprilysin [39,41,42], a key enzyme for  $\beta$ -amyloid degradation [43]. In addition, it is well-recognized that the blood–brain barrier (BBB) is compromised by HIV-1 viral proteins (for review, [44]); dysfunction which may influence  $\beta$ -amyloid homeostasis. For example, HIV-1 particles increased the release of BBB-derived extracellular vesicles and increased the  $\beta$ -amyloid cargo load in extracellular vesicles [45].

In addition to these neuropathological findings, HIV-1 Tg rats exhibited prominent alterations in the progression of temporal processing relative to control animals. In preclinical biological systems, temporal processing is often evaluated using prepulse inhibition (PPI) of the auditory startle response (ASR; [46,47]); the gap-PPI experimental paradigm utilized in the present study is based on the modification of PPI [48]. Specifically, both PPI and gap-PPI rely upon the presentation of a discrete prestimulus and a startling stimulus [49]. However, whereas the discrete prestimulus is added (e.g., tone) in PPI, the discrete prestimulus is removed (e.g., a gap in background noise) in gap-PPI. Indeed, in gap-PPI, the presentation of a discrete prestimulus 30 to 200 msec prior to the startling stimulus elicits a pronounced reduction in startle response [48]. High translational relevance (e.g., via utilization of the eyeblink startle experimental paradigm as in [50]) and the well-established neural circuitry (for review, [51]) illustrate two of the key advantages of utilizing the PPI and gap-PPI experimental paradigms.

Both the PFC and hippocampus [51], brain regions that exhibit abnormal intraneuronal  $\beta$ -amyloid accumulation in aging HIV-1 Tg rats, are fundamentally involved in the regulation of PPI. The serial neural circuit mediating PPI begins by relaying auditory input to the inferior colliculus, which subsequently innervates the superior colliculus. Sensory input from the superior colliculus is then sent to the pedunculopine tegmental nucleus (PPTg). Cholinergic projections from the PPTg to the pontine reticular nucleus are relayed to motor neurons resulting in the elicitation of a startle response. Both the ventral hippocampus [52] and PFC [53,54] send afferents to the nucleus accumbens (NAc), which subsequently innervates the PPTg. Disruption of neurotransmission in either the ventral hippocampus (e.g., [55,56]) or PFC (e.g., [57,58]) lead to prominent reductions in PPI; reductions which resemble those observed in the HIV-1 Tg rat. Given the fundamental role of  $\beta$ -amyloid in neurotransmission (for review, [59]), it is conceivable that the abnormal intraneuronal  $\beta$ -amyloid accumulation may underlie the prominent alterations in the progression of temporal processing observed in HIV-1 Tg animals.

Due to the increasing prevalence of older HIV-1 seropositive individuals, differentiating HAND from other neurodegenerative diseases, including Alzheimer's disease (AD), is a fundamental concern; the results of the present paper highlight two facets of HAND that differentiate it from AD. First, HIV-1 Tg rats and HIV-1 seropositive individuals with HAND exhibited intraneuronal  $\beta$ -amyloid accumulation in the absence of any significant extracellular  $\beta$ -amyloid plaques. In sharp contrast, one of the salient pathological features of AD is visible, neuritic extracellular plaques [60,61] comprised primarily of  $\beta$ -amyloid [62]. It is noteworthy that diffuse (rather than neuritic)  $\beta$ -amyloid plaques were previously observed in HIV-1 seropositive individuals not receiving cART treatment [63]. In the cART era, when extracellular plaques have been observed in HIV-1 seropositive, they are primarily located in the perivascular regions [37,38]; again, in sharp contrast to the location (i.e., initially in the entorhinal cortex and hippocampus; [64]) of extracellular neuritic plaques associated with AD. Second, temporal processing has been proposed as a key neurobehavioral mechanism underlying neurocognitive impairments associated with HIV-1 [65]. Cross-sectional studies have identified deficits in temporal processing and/or PPI in HIV-1 seropositive individuals with HAND [50] and multiple biological systems utilized to model HAND (e.g., HIV-1 Tg Rat [66,67]; Stereotaxic Injections of Tat [68,69]

or gp120 [70]; gp120 Transgenic Mice: [71,72]; Tat Transgenic Mice: [73]). A longitudinal study in the HIV-1 Tg rat revealed alterations in the progression of temporal processing [35,74]; the present study extends these observations, revealing their generalizability via the evaluation of temporal processing using a different experimental paradigm. With regards to AD, however, evidence for alterations in temporal processing has been inconclusive [75]. More broadly, HIV-1 and AD are differentiated by unique neurocognitive profiles, whereby HAND primarily exhibits a “subcortical” pattern (e.g., attention, executive function; for review [76]). Indeed, evaluating six cognitive measures accurately discriminates between milder forms of HAND and AD with high accuracy (i.e., 86%; [77]). There remains, however, a critical need to further delineate similarities and differences in the phenotype of HAND and AD necessitating a biological system to model HAND in older HIV-1 seropositive individuals.

Observations across a multitude of studies, including the present one, support the utility of the HIV-1 Tg rat to model HAND in older HIV-1 seropositive individuals. The HIV-1 Tg rat, originally reported by Reid et al. [33], expresses seven of the nine HIV-1 genes constitutively throughout development; the deletion of *gag* and *pol* renders the HIV-1 Tg rat non-infectious. The contemporary phenotype of the HIV-1 Tg rat, on the F344/N background strain, is healthy through advanced age, with approximately 50% of HIV-1 Tg rats surviving through 21 months of age [78]. Furthermore, HIV-1 Tg rats exhibit intact sensory (i.e., auditory, visual) and gross-motoric system function through advancing age [74] affording an opportunity to evaluate neurocognitive impairments. Indeed, cross-sectional studies have demonstrated that neurocognitive impairments observed in the HIV-1 Tg rat (e.g., attention: [79,80]; executive function: [20,79]; memory: [81–83]; preattentive processes/temporal processing: [66,67]) resemble those commonly altered in HIV-1 seropositive individuals on cART [84,85]. Longitudinal studies have further illustrated progressive neurocognitive impairments in the HIV-1 Tg rat through the functional lifespan [20,74]. Prominent sex differences in neurocognitive impairments have been observed in HIV-1 seropositive individuals, whereby female, relative to male, HIV-1 seropositive individuals exhibit greater neurocognitive impairments [86]; findings which have been recapitulated in the HIV-1 Tg rat [20,80]. With regards to potential neural mechanisms underlying HAND, the HIV-1 Tg rat exhibits prominent synaptodendritic damage in multiple brain regions (PFC: [20,21]; Nucleus Accumbens: [18,19,87]); damage which progresses through six months of age [88]. Additionally, as illustrated in the present study, the intraneuronal nature of  $\beta$ -amyloid accumulation in the HIV-1 Tg rat resembled observations in HIV-1 seropositive individuals with HAND. Collectively, the neuropathological and neurocognitive findings of the present study afford additional credence to the utility of the HIV-1 Tg rat as a biological system to model HAND in older HIV-1 seropositive individuals.

Despite the strengths of the present study, a few limitations must be acknowledged. First, the absence of matched human control autopsy brain tissue prevents the determination of whether intraneuronal  $\beta$ -amyloid accumulation in HIV-1 seropositive individuals is abnormal. Given the request for HIV-1 seropositive human autopsy brain tissue from individuals with neurocognitive impairments, we posit that intraneuronal  $\beta$ -amyloid accumulation, in the absence of prominent  $\beta$ -amyloid plaques, reflects brain pathology in the current population. Second, neuroanatomical and neurocognitive assessments were conducted in two separate cohorts of animals; synaptodendritic alterations were not evaluated in the present study. Future studies directly evaluating the relationship between  $\beta$ -amyloid accumulation, synaptodendritic alterations, and neurocognitive function are critical to further enhancing our understanding of HAND pathology.

In conclusion, potential abnormal intraneuronal  $\beta$ -amyloid accumulation supports a potential factor underlying the neural pathogenesis of HAND in the post-cART era. Aging HIV-1 Tg rats exhibited abnormal intraneuronal  $\beta$ -amyloid accumulation in both the PFC and hippocampus. Furthermore, the HIV-1 Tg rat exhibited prominent alterations in temporal processing; a cognitive process that is dependent upon intact PFC and hippocampal.



Elucidating a potential factor underlying synaptodendritic alterations in HIV-1 affords a key target for future studies evaluating novel therapeutics.

**Supplementary Materials:** The following supporting information can be downloaded at: <https://www.mdpi.com/article/10.3390/v14061268/s1>, Table S1: Information of Manhattan HIV Brain Bank participants.

**Author Contributions:** H.L. conducted the neuroanatomical assessments (i.e., IHC and DiOlistic labeling) and was a major contributor in writing the manuscript. K.A.M. performed the neurocognitive assessments (i.e., PPI), data analysis, and contributed to the writing and editing of the manuscript. B.L. assisted with tissue processing and analysis. W.H. and S.L.C. provided materials for the study and edited the manuscript. C.F.M. and R.M.B. obtained funding for the research and edited and revised the manuscript. All authors have read and agreed to the published version of the manuscript.

**Funding:** This publication was made possible by National Institutes of Health (NIH) grants MH106392, DA013137, and NS100624; along with shared resources from NIH funding through the NIMH and NINDS by the following grants: Manhattan HIV Brain Bank (MHBB) U24MH100931, Texas NeuroAIDS Research Center (TNRC) U24MH100930, and the Data Coordinating Center (DCC) U24MH100925. The publication contents are solely the responsibility of the authors and do not necessarily represent the official view of the NNTC or NIH.

**Institutional Review Board Statement:** The protocols were approved by the Institutional Animal Care and Use Committee (IACUC) at the University of South Carolina (Federal Assurance #D16-00028) and Seton Hall University (Federal Assurance #D16-00291).

**Data Availability Statement:** All data are available in the main text.

**Conflicts of Interest:** The authors declare no conflict of interest.

## References

1. Romley, J.A.; Juday, T. Early HIV treatment led to life expectancy gains valued at \$80 billion for people infected in 1996–2009. *Health Aff.* **2014**, *33*, 370–377. [[CrossRef](#)] [[PubMed](#)]
2. Teeraananchai, S.; Chaivooth, S. Life expectancy after initiation of combination antiretroviral therapy in Thailand. *Antivir. Ther.* **2017**, *22*, 393–402. [[CrossRef](#)]
3. HIV and Aging. Available online: [https://www.unaids.org/en/resources/documents/2013/20131101\\_JC2563\\_hiv-and-aging](https://www.unaids.org/en/resources/documents/2013/20131101_JC2563_hiv-and-aging) (accessed on 14 December 2021).
4. Smit, M.; Brinkman, K. Future challenges for clinical care of an ageing population infected with HIV: A modelling study. *Lancet Infect Dis.* **2015**, *15*, 810–818. [[CrossRef](#)]
5. Valcour, V.; Shikuma, C. Higher frequency of dementia in older HIV-1 individuals: The Hawaii Aging with HIV-1 Cohort. *Neurology* **2004**, *63*, 822–827. [[CrossRef](#)]
6. Becker, J.T.; Lopez, O.L. Prevalence of cognitive disorders differs as a function of age in HIV virus infection. *AIDS* **2004**, *18*, S11–S18. [[CrossRef](#)]
7. Vance, D.E.; Wadley, V.G. Cognitive and Everyday Functioning in Older and Younger Adults with and without HIV. *Clin. Gerontol.* **2011**, *34*, 413–426. [[CrossRef](#)] [[PubMed](#)]
8. Moore, D.J.; Masliah, E. Cortical and subcortical neurodegeneration is associated with HIV neurocognitive impairment. *AIDS* **2006**, *20*, 879–887. [[CrossRef](#)] [[PubMed](#)]
9. Ellis, R.; Langford, D.; Masliah, E. HIV and antiretroviral therapy in the brain: Neuronal injury and repair. *Nat. Rev. Neurosci.* **2007**, *8*, 33–44. [[CrossRef](#)] [[PubMed](#)]
10. Gelman, B.B.; Nguyen, T.P. Synaptic proteins linked to HIV-1 infection and immunoproteasome induction: Proteomic analysis of human synaptosomes. *J. Neuroimmune Pharmacol.* **2010**, *5*, 92–102. [[CrossRef](#)] [[PubMed](#)]
11. Desplats, P.; Dumaop, W. Molecular and pathologic insights from latent HIV-1 infection in the human brain. *Neurology* **2013**, *80*, 1415–1423. [[CrossRef](#)] [[PubMed](#)]
12. Weiss, J.J.; Calvi, R. Preliminary in vivo evidence of reduced synaptic density in human immunodeficiency virus (HIV) despite antiretroviral therapy. *Clin. Infect Dis.* **2021**, *73*, 1404–1411. [[CrossRef](#)]
13. Avdoshina, V.; Mahoney, M. HIV influences microtubule associated protein-2: Potential marker of HIV-associated neurocognitive disorders. *AIDS* **2020**, *34*, 979–988. [[CrossRef](#)]
14. Fitting, S.; Xu, R. Interactive comorbidity between opioid drug abuse and HIV-1 Tat: Chronic exposure augments spine loss and sublethal dendritic pathology in striatal neurons. *Am. J. Pathol.* **2010**, *177*, 1397–1410. [[CrossRef](#)]
15. Fitting, S.; Ignatowska-Jankowska, B.M. Synaptic dysfunction in the hippocampus accompanies learning and memory deficits in human immunodeficiency virus type-1 Tat transgenic mice. *Biol. Psychiatry* **2013**, *73*, 443–453. [[CrossRef](#)] [[PubMed](#)]

16. Kang, Y.J.; Digicaylioglu, M. Erythropoietin plus insulin-like growth factor-I protects against neuronal damage in a murine model of human immunodeficiency virus-associated neurocognitive disorders. *Ann. Neurol.* **2010**, *68*, 342–352. [[CrossRef](#)] [[PubMed](#)]
17. Speidell, A.; Asuni, G.P. Up-regulation of the p75 neurotrophin receptor is an essential mechanism for HIV-gp120 mediated synaptic loss in the striatum. *Brain Behav. Immun.* **2020**, *89*, 371–379. [[CrossRef](#)] [[PubMed](#)]
18. Roscoe, R.F., Jr.; Mactutus, C.F. HIV-1 Transgenic female rat: Synaptodendritic alterations of medium spiny neurons in the nucleus accumbens. *J. Neuroimmune Pharmacol.* **2014**, *9*, 642–653. [[CrossRef](#)] [[PubMed](#)]
19. McLaurin, K.A.; Cook, A.K. Synaptic Connectivity in Medium Spiny Neurons of the Nucleus Accumbens: A Sex-Dependent Mechanism Underlying Apathy in the HIV-1 Transgenic Rat. *Front. Behav. Neurosci.* **2018**, *12*, 285. [[CrossRef](#)] [[PubMed](#)]
20. McLaurin, K.A.; Li, H. Disruption of timing: NeuroHIV progression in the post-cART era. *Sci. Rep.* **2019**, *9*, 827. [[CrossRef](#)] [[PubMed](#)]
21. Festa, L.K.; Irollo, E. CXCL12-induced rescue of cortical dendritic spines and cognitive flexibility. *Elife* **2020**, *9*, e49717. [[CrossRef](#)]
22. Li, H.; McLaurin, K.A. Microglial HIV-1 expression: Role in HIV-1 associated neurocognitive disorders. *Viruses* **2021**, *13*, 924. [[CrossRef](#)] [[PubMed](#)]
23. Aksenov, M.Y.; Aksenova, M.V. HIV-1 protein-mediated amyloidogenesis in rat hippocampal cell cultures. *Neurosci. Lett.* **2010**, *475*, 174–178. [[CrossRef](#)] [[PubMed](#)]
24. Hategan, A.; Masliah, E. HIV and Alzheimer's disease: Complex interactions of HIV-Tat with amyloid beta peptide and Tau protein. *J. Neurovirol.* **2019**, *25*, 648–660. [[CrossRef](#)] [[PubMed](#)]
25. Shankar, G.M.; Bloodgood, B.L. Natural oligomers of the Alzheimer amyloid-beta protein induce reversible synapse loss by modulating an NMDA-type glutamate receptor-dependent signaling pathway. *J. Neurosci.* **2007**, *27*, 2866–2875. [[CrossRef](#)] [[PubMed](#)]
26. Tackenberg, C.; Brandt, R. Divergent pathways mediate spine alterations and cell death induced by amyloid- $\beta$ , wild-type tau, and R406W tau. *J. Neurosci.* **2009**, *29*, 14439–14450. [[CrossRef](#)]
27. Chen, G.F.; Xu, T.H. Amyloid beta: Structure, biology and structure-based therapeutic development. *Acta Pharmacol. Sin.* **2017**, *38*, 1205–1235. [[CrossRef](#)] [[PubMed](#)]
28. Takami, M.; Nagashima, Y. Gamma-secretase: Successive tripeptide and tetrapeptide release from the transmembrane domain of beta-carboxyl terminal fragment. *J. Neurosci.* **2009**, *29*, 13042–13052. [[CrossRef](#)]
29. Olsson, F.; Schmidt, S. Characterization of intermediate steps in amyloid beta (A $\beta$ ) production under near-native conditions. *J. Biol. Chem.* **2014**, *289*, 1540–1550. [[CrossRef](#)]
30. Mori, H.; Takio, K. Mass spectrometry of purified amyloid beta protein in Alzheimer's disease. *J. Biol. Chem.* **1992**, *267*, 17082–17086. [[CrossRef](#)]
31. Jarrett, J.T.; Berger, E.P. The carboxy terminus of the beta amyloid protein is critical for the seeding of amyloid formation: Implications for the pathogenesis of Alzheimer's disease. *Biochemistry* **1993**, *32*, 4693–4697. [[CrossRef](#)]
32. Roher, A.E.; Lowenson, J.D. beta-Amyloid-(1-42) is a major component of cerebrovascular amyloid deposits: Implications for the pathology of Alzheimer disease. *Proc. Natl. Acad. Sci. USA* **1993**, *90*, 10836–10840. [[CrossRef](#)] [[PubMed](#)]
33. Reid, W.; Sadowska, M. An HIV-1 transgenic rat that develops HIV-related pathology and immunologic dysfunction. *Proc. Natl. Acad. Sci. USA* **2001**, *98*, 9271–9276. [[CrossRef](#)]
34. Li, H.; McLaurin, K.A.; Mactutus, C.F.; Booze, R.M. Ballistic Labeling of Pyramidal Neurons in Brain Slices and in Primary Cell Culture. *J. Vis. Exp.* **2020**, *158*, 60989. [[CrossRef](#)] [[PubMed](#)]
35. McLaurin, K.A.; Booze, R.M.; Mactutus, C.F. Progression of temporal processing deficits in the HIV-1 transgenic rat. *Sci. Rep.* **2016**, *6*, 32831. [[CrossRef](#)]
36. Brodmann, K. *Vergleichende Lokalisationslehre der Grosshirnrinde in Inren Prinzipien Dargestellt auf Grund des Zellenbaues*; Leipzig: Barth, Germany, 1909.
37. Green, D.A.; Masliah, E. Brain deposition of beta-amyloid is a common pathologic feature in HIV positive patients. *AIDS* **2005**, *19*, 407–411. [[CrossRef](#)]
38. Achim, C.L.; Adame, A.; Dumaop, W.; Everall, I.P.; Masliah, E. Increased accumulation of intraneuronal amyloid beta in HIV-infected patients. *J. Neuroimmune Pharmacol.* **2009**, *4*, 190–199. [[CrossRef](#)]
39. Rempel, H.C.; Pulliam, L. HIV-1 Tat inhibits neprilysin and elevates amyloid beta. *AIDS* **2005**, *19*, 127–135. [[CrossRef](#)] [[PubMed](#)]
40. András, I.E.; Eum, S.Y. HIV-1-induced amyloid beta accumulation in brain endothelial cells is attenuated by simvastatin. *Mol. Cell Neurosci.* **2010**, *43*, 232–243. [[CrossRef](#)] [[PubMed](#)]
41. Daily, A.; Nath, A. Tat peptides inhibit neprilysin. *J. Neurovirol.* **2006**, *12*, 153–160. [[CrossRef](#)] [[PubMed](#)]
42. Chen, Q.; Wu, Y. Rho-kinase inhibitor hydroxyfasudil protects against HIV-1 Tat-induced dysfunction of tight junction and neprilysin/A $\beta$  transfer receptor expression in mouse brain microvessels. *Mol. Cell Biochem.* **2021**, *476*, 2159–2170. [[CrossRef](#)] [[PubMed](#)]
43. Huang, J.; Guan, H. Estrogen regulates neprilysin activity in rat brain. *Neuroscience Lett.* **2004**, *367*, 85–87. [[CrossRef](#)] [[PubMed](#)]
44. Atluri, V.S.R.; Hidalgo, M. Effect of human immunodeficiency virus on blood-brain barrier integrity and function: An update. *Front Cell Neurosci.* **2015**, *9*, 212. [[CrossRef](#)] [[PubMed](#)]
45. András, I.E.; Leda, A. Extracellular vesicles of the blood-brain barrier: Role in the HIV-1 associated amyloid beta pathology. *Mol. Cell Neurosci.* **2017**, *79*, 12–22. [[CrossRef](#)] [[PubMed](#)]



46. Hoffman, H.S.; Searle, J.L. Acoustic variables in the modification of startle reaction in the rat. *J. Comp. Physiol. Psychol.* **1965**, *60*, 53–58. [[CrossRef](#)] [[PubMed](#)]
47. Ison, J.R.; Hammond, G.R. Modification of the startle reflex in the rat by changes in the auditory and visual environments. *J. Comp. Physiol. Psychol.* **1971**, *75*, 435–452. [[CrossRef](#)]
48. Ison, J.R.; Agrawal, P. Changes in temporal acuity with age and with hearing impairment in the mouse: A study of the acoustic startle reflex and its inhibition by brief decrements in noise level. *J. Acoust. Soc. Am.* **1998**, *104*, 1696–1704. [[CrossRef](#)]
49. Hoffman, H.S.; Ison, J.R. Reflex modification in the domain of startle: I. Some empirical findings and their implications for how the nervous system processes sensory input. *Psychol. Rev.* **1980**, *87*, 175–189. [[CrossRef](#)]
50. Minassian, A.; Henry, B.L. Prepulse inhibition in HIV-associated Neurocognitive disorders. *J. Int. Neuropsychol. Soc.* **2013**, *7*, 255–263. [[CrossRef](#)]
51. Koch, M. The neurobiology of startle. *Prog. Neurobiol.* **1999**, *59*, 107–128. [[CrossRef](#)]
52. Groenewegen, H.J.; Vermeulen-Van der Zee, E. Organization of the projections from the subiculum to the ventral striatum in the rat. A study using anterograde transport of Phaseolus vulgaris leucoagglutinin. *Neuroscience* **1987**, *23*, 103–120. [[CrossRef](#)]
53. Berendse, H.W.; Galis-de Graaf, Y. Topographical organization and relationship with ventral striatal compartments of prefrontal corticostriatal projections in the rat. *J. Comp. Neurol.* **1992**, *316*, 314–347. [[CrossRef](#)] [[PubMed](#)]
54. Brog, J.S.; Salyapongse, A. The patterns of afferent innervation of the core and shell in the “accumbens” part of the rat ventral striatum: Immunohistochemical detection of retrogradely transported fluoro-gold. *J. Comp. Neurol.* **1993**, *338*, 255–278. [[CrossRef](#)] [[PubMed](#)]
55. Wan, F.J.; Caine, S.B. The ventral subiculum modulation of prepulse inhibition is not mediated via dopamine D<sub>2</sub> or nucleus accumbens non-NMDA glutamate receptor activity. *Eur. J. Pharmacol.* **1996**, *314*, 9–18. [[CrossRef](#)]
56. Zhang, W.N.; Bast, T. Prepulse inhibition in rats with temporary inhibition/inactivation of ventral or dorsal hippocampus. *Pharmacol. Biochem. Behav.* **2002**, *73*, 929–940. [[CrossRef](#)]
57. Bubser, M.; Koch, M. Prepulse inhibition of the acoustic startle response of rats is reduced by 6-hydroxydopamine lesions of the medial prefrontal cortex. *Psychopharmacology* **1994**, *113*, 487–492. [[CrossRef](#)]
58. Fitting, S.; Booze, R.M. Neonatal intrahippocampal glycoprotein 120 injection: The role of dopaminergic alterations in prepulse inhibition in adult rats. *J. Pharmacol. Exp. Ther.* **2006**, *318*, 1352–1358. [[CrossRef](#)]
59. Fagiani, F.; Lanni, C. (Dys)regulation of synaptic activity and neurotransmitter release by  $\beta$ -amyloid: A look beyond Alzheimer’s disease pathogenesis. *Front. Mol. Neurosci.* **2021**, *14*, 635880. [[CrossRef](#)]
60. Alzheimer, A. Über eine eigenartige Erkrankung der Hirnrinde. *Z. Psychiatr. Psychiatr.-Gerichtl. Med.* **1907**, *64*, 146–148.
61. Tomlinson, B.E.; Blessed, G. Observations on the brains of demented old people. *J. Neurol. Sci.* **1970**, *11*, 205–242. [[CrossRef](#)]
62. Glenner, G.G.; Wong, C.W. Alzheimer’s disease: Initial report of the purification and characterization of a novel cerebrovascular amyloid protein. *Biochem. Biophys. Res. Commun.* **1984**, *120*, 885–890. [[CrossRef](#)]
63. Esiri, M.M.; Biddolph, S.C. Prevalence of Alzheimer plaques in AIDS. *J. Neurol. Neurosurg. Psychiatry* **1998**, *65*, 29–33. [[CrossRef](#)] [[PubMed](#)]
64. Van Hoesen, G.W.; Hyman, B.T. Entorhinal cortex pathology in Alzheimer’s disease. *Hippocampus* **1991**, *1*, 1–8. [[CrossRef](#)] [[PubMed](#)]
65. McLaurin, K.A.; Mactutus, C.F. An empirical mediation analysis of mechanisms underlying HIV-1-Associated neurocognitive disorders. *Brain Res.* **2019**, *1724*, 146436. [[CrossRef](#)] [[PubMed](#)]
66. Moran, L.M.; Booze, R.M. Time and time again: Temporal processing demands implicate perceptual and gating deficits in the HIV-1 transgenic rat. *J. Neuroimmune Pharmacol.* **2013**, *8*, 988–997. [[CrossRef](#)] [[PubMed](#)]
67. McLaurin, K.A.; Booze, R.M. Temporal processing demands in the HIV-1 transgenic rat: Amodal gating and implications for diagnosis. *Int. J. Dev. Neurosci.* **2017**, *57*, 12–20. [[CrossRef](#)]
68. Fitting, S.; Booze, R.M. Neonatal hippocampal Tat injections: Developmental effects on prepulse inhibition (PPI) of the auditory startle response. *Int. J. Dev. Neurosci.* **2006**, *24*, 275–283. [[CrossRef](#)]
69. Fitting, S.; Booze, R.M. Intrahippocampal injections of Tat: Effects on prepulse inhibition of the auditory startle response in adult male rats. *Pharmacol. Biochem. Behav.* **2006**, *84*, 189–196. [[CrossRef](#)]
70. Fitting, S.; Booze, R.M. Neonatal intrahippocampal gp120 injection: An examination early in development. *Neurotoxicology* **2007**, *28*, 101–107. [[CrossRef](#)]
71. Henry, B.; Geyer, M.A. Prepulse inhibition in HIV-1 gp120 transgenic mice after withdrawal from chronic methamphetamine. *Behav. Pharmacol.* **2014**, *25*, 12–22. [[CrossRef](#)]
72. Bachis, A.; Forcelli, P. Expression of gp120 in mice evokes anxiety behavior: Co-occurrence with increased dendritic spines and brain-derived neurotrophic factor in the amygdala. *Brain Behav. Immun.* **2016**, *54*, 170–177. [[CrossRef](#)]
73. Paris, J.J.; Singh, H.D. Exposure to HIV-1 Tat in brain impairs sensorimotor gating and activates microglia in limbic and extralimbic brain regions of male mice. *Behav. Brain Res.* **2015**, *291*, 209–218. [[CrossRef](#)]
74. McLaurin, K.A.; Booze, R.M. Evolution of the HIV-1 transgenic rat: Utility in assessing the progression of HIV-1-associated neurocognitive disorders. *J. Neurovirol.* **2018**, *24*, 229–245. [[CrossRef](#)] [[PubMed](#)]
75. Hejl, A.M.; Glenthøj, B. Prepulse inhibition in patients with Alzheimer’s disease. *Neurobiol. Aging* **2004**, *25*, 1045–1050. [[CrossRef](#)]
76. Milanini, B.; Valcour, V. Differentiating HIV-associated neurocognitive disorders from Alzheimer’s disease: An emerging issue in geriatric neuroHIV. *Curr. HIV/AIDS Rep.* **2017**, *14*, 123–132. [[CrossRef](#)] [[PubMed](#)]

77. Milanini, B. Discriminant analysis of neuropsychological testing differentiates HIV-associated neurocognitive disorder from mild cognitive impairment due to Alzheimer's disease. In Proceedings of the International Society of NeuroVirology, Toronto, Canada, 25–28 October 2016.
78. Peng, J.; Vigorito, M. The HIV-1 transgenic rat as a model for HIV-1 infected individuals on HAART. *J. Neuroimmunol.* **2010**, *218*, 94–101. [[CrossRef](#)]
79. Moran, L.M.; Booze, R.M. Modeling deficits in attention, inhibition, and flexibility in HAND. *J. Neuroimmune Pharmacol.* **2014**, *9*, 508–521. [[CrossRef](#)] [[PubMed](#)]
80. McLaurin, K.A.; Booze, R.M. Sex matters: Robust sex differences in signal detection in the HIV-1 transgenic rat. *Front. Behav. Neurosci.* **2017**, *11*, 212. [[CrossRef](#)] [[PubMed](#)]
81. Vigorito, M.; LaShomb, A.L. Spatial learning and memory in HIV-1 transgenic rats. *J. Neuroimmune Pharmacol.* **2007**, *2*, 319–328. [[CrossRef](#)]
82. Lashomb, A.L.; Vigorito, M. Further characterization of the spatial learning deficit in the human immunodeficiency virus-1 transgenic rat. *J. Neurovirol.* **2009**, *15*, 14–24. [[CrossRef](#)]
83. Repunte-Canonigo, V.; Lafebvre, C. Gene expression changes consistent with neuroAIDS and impaired working memory in HIV-1 transgenic rats. *Mol. Neurodegener.* **2014**, *9*, 26. [[CrossRef](#)]
84. Heaton, R.K.; Franklin, D.R. HIV-associated neurocognitive disorders before and during the era of combination antiretroviral therapy: Differences in rates, nature, and predictors. *J. Neurovirol.* **2011**, *17*, 3–16. [[CrossRef](#)] [[PubMed](#)]
85. Cysique, L.A.; Maruff, P. Prevalence and pattern of neuropsychological impairment in human immunodeficiency virus-infected/acquired immunodeficiency syndrome (HIV/AIDS) patients across pre- and post-highly active antiretroviral therapy eras: A combined study of two cohorts. *J. Neurovirol.* **2004**, *10*, 350–357. [[CrossRef](#)] [[PubMed](#)]
86. Rubin, L.H.; Neigh, G.N.; Sundermann, E.E.; Xu, Y.; Scully, E.P.; Maki, P.M. Sex Differences in Neurocognitive Function in Adults with HIV: Patterns, Predictors, and Mechanisms. *Curr. Psychiatry Rep.* **2019**, *21*, 94. [[CrossRef](#)] [[PubMed](#)]
87. McLaurin, K.A.; Bertrand, S.J. S-Equol mitigates motivational deficits and dysregulation associated with HIV-1. *Sci. Rep.* **2021**, *11*, 11870. [[CrossRef](#)]
88. McLaurin, K.A.; Li, H. Neurodevelopmental processes in the prefrontal cortex derailed by chronic HIV-1 viral protein exposure. *Cells* **2021**, *10*, 3037. [[CrossRef](#)] [[PubMed](#)]